Hindawi Publishing Corporation
Shock and Vibration
Volume 2014, Article ID 172570, 9 pages
http://dx.doi.org/10.1155/2014/172570

*Research Article*

# Experimental Verifications of Vibration Suppression for a Smart Cantilever Beam with a Modified Velocity Feedback Controller

**Ting Zhang,[1] Hong Guang Li,[1] Guo Ping Cai,[2] and Fu Cai Li[1]**

[1] *The State Key Laboratory of Mechanical System and Vibration, Shanghai Jiao Tong University, Shanghai 200240, China*
[2] *Department of Engineering Mechanics, Shanghai Jiao Tong University, Shanghai 200240, China*

Correspondence should be addressed to Hong Guang Li; hgli@sjtu.edu.cn

Received 5 August 2013; Accepted 21 January 2014; Published 27 February 2014

Academic Editor: Mohammad Elahinia



This paper presents various experimental verifications for the theoretical analysis results of vibration suppression to a smart flexible beam bonded with a piezoelectric actuator by a velocity feedback controller and an extended state observer (ESO). During the state feedback control (SFC) design process for the smart flexible beam with the pole placement theory, in the state feedback gain matrix, the velocity feedback gain is much more than the displacement feedback gain. For the difference between the velocity feedback gain and the displacement feedback gain, a modified velocity feedback controller is applied based on a dynamical model with the Hamilton principle to the smart beam. In addition, the feedback velocity is attained with the extended state observer and the displacement is acquired by the foil gauge on the root of the smart flexible beam. The control voltage is calculated by the designed velocity feedback gain multiplied by the feedback velocity. Through some experiment verifications for simulation results, it is indicated that the suppressed amplitude of free vibration is up to 62.13% while the attenuated magnitude of its velocity is up to 61.31%. Therefore, it is demonstrated that the modified velocity feedback control with the extended state observer is feasible to reduce free vibration.

## 1. Introduction

In recent years, a smart system, which consists of a cantilever beam bonded with a piezoelectric actuator, has drawn much interest of many researchers [1–5]. At the same time, the controller designs based on positioning control and vibration suppression of the smart system have attracted wide attention around the world [6]. Especially for dynamic modeling task and vibration reduction work of a smart cantilever beam with piezoelectric materials, there have been lots of studies on suppressing vibration with a designed controller [7]. For example, a full-order model is developed using assumed model expansion and the Lagrangian approach for a flexible cantilever beam bonded with a PZT patch to control a base motion [8], a finite element model of the three-layered smart beam is utilized to reduce vibration by a velocity feedback controller [9], and the multimodal vibration suppression of a smart flexible cantilever beam with piezoceramic actuator and sensor by using a pole placement method is proposed [10].

As for adopted control law to suppress vibration of mechanical system, in the past several years, many researchers have committed to the work on vibration control of a smart beam with piezoelectric sensor and actuator by a variety of controllers [11]. An acceleration sensor based on proportional feedback control algorithm and sliding mode variable structure control algorithm with phase shifting technology is proposed for suppressing the first two bending mode vibrations of a beam [12]. A modified acceleration feedback control method is developed for active vibration control of the aerospace structures [13]. A linear quadratic regulator (LQR) controller is adopted to achieve vibration suppression of the laminated smart beam [14]. A controller is designed using proportion-integral-derivative theory with output feedback to control the vibrations of any real-life system [15]. A sliding mode control (SMC) with backstepping technique is employed to control the attitude motion of a spacecraft [16]. The vibration suppression is achieved through a combined scheme of PD-based hub motion control and a PZT actuator controller that is a composite of linear and

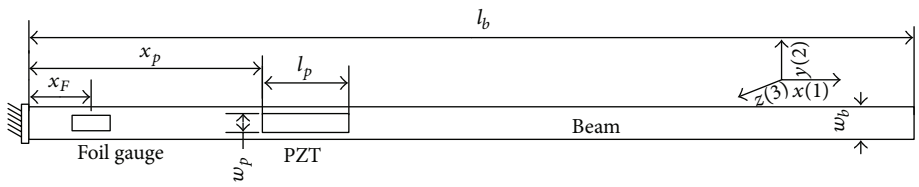


Figure 1: A cantilevered beam bonded with a piezoelectric actuator.

angular velocity feedback controllers [17]. Nonaxisymmetric vibrations of a clamped-free cylindrical shell partially treated with a laminated PVDF actuator are controlled using an adaptive filtered-X least mean square algorithm [18]. A modal velocity feedback control method is applied to suppress the undesirable vibration [19]. An improved version of the previously developed synchronized switch damping on voltage (SSDV) approach [20] and an adaptive semiactive SSDV method through the LMS algorithm [21] are proposed and are applied to the vibration control of a composite beam. An adaptive law is adopted for the purpose of providing an additional force to control frequency changes caused by broadband vibrations [22]. A novel approach is developed for achieving a high performance piezoelectric vibration absorber [23]. A robust adaptive sliding mode attitude controller is designed to control system for rotation maneuver and vibration suppression of a flexible spacecraft [24]. However, there is lack of a simplified model to suppress vibration for a smart cantilever beam with an effective controller.

In this paper, a dynamical model of a smart beam is proposed by combining the Hamilton principle and the assumed mode method [25]. In addition, based on the dynamical model, a controller with the velocity feedback control [26–28] through the pole placement theory is designed to suppress free vibration of the smart beam. In the velocity feedback control design process, the feedback velocity is observed through the extended state observer [29–31] with the output displacement of the smart beam sensed by foil gauge. In a word, a dynamical model is constructed to design the velocity feedback gain and suppress the first-order free vibration of the smart beam with the extended state observer.

The rest of this paper is organized as follows. A dynamical model for the smart system is constructed in Section 2. An extended state observer and a velocity feedback controller are designed for the purpose of vibration suppression in Section 3. Some simulations and experiments are performed to verify the vibration reduction effectiveness for the smart beam by the velocity feedback controller in Section 4. Finally, some conclusions are given in Section 5.

## 2. Dynamic Modeling for Smart System

A cantilevered beam bonded with a piezoelectric actuator and a foil gauge is shown in Figure 1. The piezoelectric actuator and the foil gauge are placed on the middle and the root of the smart beam, respectively. When the end tip of the smart beam is subjected to an external disturbance, the piezoelectric actuator is activated with the control voltage generated by a designed controller to suppress the disturbance or vibration. However, before that, the dynamical model for the actuating system must be proposed using energy conservation law.

As shown in Figure 1, the displacement $u$ of the smart beam can be written as

$$\begin{aligned} u_1 &= u_x(x,z,t) - z\psi_x(x,z,t), \\ u_3 &= u_z(x,z,t), \end{aligned} \tag{1}$$

where $\psi_x(x,z,t) = (\partial u_z(x,z,t))/\partial x$.

At the same time, the strain $s$ and stress $S$ should be expressed as

$$\begin{aligned} s_1 &= \frac{\partial u_x}{\partial x} - z\frac{\partial \psi_x}{\partial x}, \\ S_1 &= c s_1, \end{aligned} \tag{2}$$

where $c$ represents the elastic stiffness constant.

Moreover, the linear constitutive equations of piezoelectric actuator have been widely used as

$$\begin{aligned} S_1 &= c_{11}^D s_1 - h_{31} D_3, \\ E_3 &= -h_{31} s_1 + \beta_{33}^x D_3, \end{aligned} \tag{3}$$

where $E$, $D$, and $\varepsilon$ represent electric field, electric displacement, and free dielectric constant, respectively; $h$ and $\beta$ represent piezoelectric stiffness constant and free dielectric isolation rate, respectively.

Furthermore, the smart system's dynamics model can then be derived using Hamilton's principle and the assumed mode method. In this paper, the former first mode of the elastic beam modes is adopted for discretization. Therefore, the displacement of $z$ direction can be expressed as

$$u_z(x,t) = \phi(x) \cdot q(t), \tag{4}$$

wherein $\phi(x)$ represents the assumed mode vector and $q(t)$ is the generalized mechanical displacement vector.

And in (4), the assumed mode is

$$\begin{aligned} \phi(x) = {} & \cosh(s_b) - \cos(s_b x) \\ & - \frac{\sinh(s_b l_b) - \sin(s_b l_b)}{\cosh(s_b l_b) + \cos(s_b l_b)} (\sinh(s_b x) - \sin(s_b x)), \end{aligned} \tag{5}$$

where $s_b$ is the eigenvalue of the elastic beam, $l_b$ is the length of beam, and $s_b l_b = 1.8751$.

Owing to (1), (2), and (4), the strain $s_1$ is expressed as

$$s_1 = -h_p \frac{\partial^2 \phi}{\partial x^2} q = Bq, \tag{6}$$

where $B$ is specified in the appendix.

Therefore, the kinetic energy $E_k$, the potential energy $E_p$, and the virtual work $W$ of the smart cantilevered beam are described as follows.

First the kinetic energy term $E_k$ is written as

$$\begin{aligned} E_k &= \frac{1}{2}\dot{q}\left(\int_0^{h_b}\int_0^{l_b} \rho_b w_b \phi^2 dx\, dz\right)\dot{q} \\ &\quad + \frac{1}{2}\dot{q}\left(\int_{h_b}^{h_b+h_p}\int_{x_p}^{x_p+l_p} \rho_p w_p \phi^2 dx\, dz\right)\dot{q} = \frac{1}{2}m(\dot{q})^2, \end{aligned} \tag{7}$$

wherein subscripts $b$ and $p$ refer to the beam and the piezoelectric actuator, respectively. $h$, $l$, $\rho$, $w$, and $x_p$ are height, length, density, width, and the location of piezoelectric actuator with respect to the fixed end of beam.

Then, assuming that $D = Q/A_p$, $Q$ is charge and $A_p$ is the cross-section area of piezoelectric actuator; the elastic, electrical, and thermal potential energy term $E_p$ is given as

$$\begin{aligned} E_p &= \frac{1}{2}\int_V (S_1 s_1 + E_3 D_3)\, dV + \frac{1}{2} q \int_0^{l_b} E_b I_b \left(\frac{\partial^2 \phi}{\partial x^2}\right)^2 q \\ &= \frac{1}{2}\int_V \left[\left(c_{11}^D s_1 - h_{31} D_3\right) s_1 + \left(-h_{31} s_1 + \beta_{33}^x D_3\right) D_3\right] dV \\ &\quad + \frac{1}{2}\left(\int_0^{l_b} E_b I_b \left(\frac{\partial^2 \phi}{\partial x^2}\right)^2 dx\right) q^2 \\ &= \frac{1}{2} k_{qq} q^2 + Q k_{Qq} q + \frac{1}{2} k_{QQ} Q^2, \end{aligned} \tag{8}$$

where $E_b$ and $I_b$ are the elastic modulus and the moment of inertia of beam, respectively, and the corresponding matrices or vectors are specified in the appendix.

Finally, the virtual work $W$ done by external force $f$, the beam's damping $c_b$, and the voltage $V$ applied on the piezoelectric actuator are expressed as

$$\begin{aligned} \delta W &= \int_0^{l_b} f \delta u_z dx - \int_0^{l_b} c_b \dot{u}_z \delta u_z dx + \int_{x_p}^{x_{p+}l_b} \frac{V}{h_p} \delta Q\, dx \\ &= \left\{\left(\int_0^{l_b} f\phi\, dx\right)\delta q - \left(\int_0^{l_b} c_b \phi^2 dx\right)\dot{q}\delta q \right. \\ &\quad \left. + \left(\int_{x_p}^{x_p+l_p} \frac{V}{h_p} dx\right)\delta Q\right\} \\ &= \alpha f \delta q - c\dot{q}\delta q + \gamma V \delta Q, \end{aligned} \tag{9}$$

where $A_b$ is the cross-section area of beam and the corresponding matrices or vectors are specified in the appendix.

Moreover, Hamilton's principle is

$$\begin{aligned} \delta J(q,\phi) &= \delta \int_{t_0}^{t_f} \left(L(q,Q;t) + W\right) dt \\ &= \delta \int_{t_0}^{t_f} \left(E_k - E_p + W\right) dt = 0. \end{aligned} \tag{10}$$

Substituting (7), (8), and (9) into (10), then

$$\begin{aligned} &m\ddot{q}\delta q + k_{qq} q \delta q + k_{Qq} q \delta Q + k_{Qq} Q \delta q \\ &\quad + k_{QQ} Q \delta Q - \left(\alpha f \delta q - c\dot{q}\delta q + \gamma V \delta Q\right) \\ &= \left(m\ddot{q} + c\dot{q} + k_{qq} q + k_{Qq} Q - \alpha f\right)\delta q \\ &\quad + \left(k_{Qq} q + k_{QQ} Q - \gamma V\right)\delta Q = 0. \end{aligned} \tag{11}$$

Therefore, from (11), the dynamical model of the smart system is obtained as

$$\begin{aligned} m\ddot{q} + c\dot{q} + k_{qq} q + k_{Qq} Q &= \alpha f, \\ k_{Qq} q + k_{QQ} Q &= \gamma V, \end{aligned} \tag{12}$$

where the corresponding parameters are specified in the appendix.

Due to (6), the output displacement $u_z$ at $x_f$ along the $z$ direction in Figure 1 is derived as

$$u_z = l_b s_1 = B\left(x_f\right) l_b q. \tag{13}$$

Finally, when external force $f$ is zero, (12) is transformed into

$$\ddot{u}_z = -2\xi\omega\dot{u}_z - \omega^2 u_z + bV, \tag{14}$$

where $\omega = \sqrt{(k_{qq} - k_{Qq}^2/k_{QQ})/m}$, $\xi = c/2m\omega$, and $b = (\gamma k_{Qq} l_b B(x_f))/k_{QQ}$.

The verification analyses of model (14) are implemented with some necessary simulations and experiments through applying a sinusoidal voltage at different frequency ($150 \times \sin(2\pi f \times t)$ and f is frequency and $t$ is time). In addition, the related geometric and mechanical parameters about simulation are given in Table 1. From Figure 2, it is obvious that the simulation curve from (14) fits in well with the experiment data. Furthermore it is informed that the first natural frequency is about 1.556 Hz and its corresponding maximum amplitude of harmonic vibration is $1.518 \times 10^{-5}$ m. Therefore, the theoretical model (14) can almost describe the harmonic characteristics of smart beam from experiment.

## 3. Observer and Controller Design

Based on above the proposed dynamical model for the smart beam, in the section, an observer and a controller are designed to suppress free vibration from the end tip of beam. Moreover, the observer is employed with the extended state observer (ESO). The ESO has advantages of not only observing high-order states of the system but also filtering

Table 1: System parameters used in simulations.

| Beam parameters | | |
|---|---|---|
| $l_b = 0.92$ m | $w_b = 0.04$ m | $h_b = 0.0032$ m |
| $\rho_b = 7.84 \times 10^3$ kg/m$^3$ | $Y_b = 2.0 \times 10^3$ N/m$^2$ | $c_b = 0.01$ |
| **Piezoelectric parameters** | | |
| $l_p = 0.05$ m | $w_p = 0.034$ m | $h_p = 0.00025$ m |
| $\rho_p = 7.8 \times 10^3$ kg/m$^3$ | $Y_p = 2.1 \times 10^3$ N/m$^2$ | $d_{31} = 2.2 \times 10^{-11}$ C/N |
| $c_{11}^D = 10.64 \times 10^{10}$ N/m$^2$ | $h_{31} = -1.35 \times 10^9$ V/m | $x_p = 0.085$ m |

Table 2: Corresponding parameters of observer and controller.

| Observer | | | Controller | |
|---|---|---|---|---|
| $r$ | $h$ | $h_1$ | $k_1$ | $k$ |
| 1000 | 0.001 | 0.03 | $2.3439 \times 10^3$ | 75.3672 |

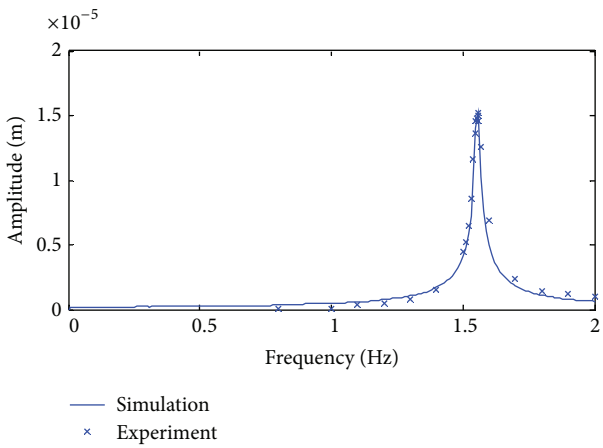


Figure 2: Amplitude-frequency property.

noise which is caused by measurement of experiment. In addition, the control law is adopted with the state feedback control through the pole placement theory. However, in the design process, it is found that the velocity feedback gain is much more than the displacement feedback one. Therefore a simplified state feedback controller, namely, a modified velocity feedback controller, is designed to attenuate the free vibration of the smart beam.

*3.1. Observer Design.* To achieve the first-order state (velocity) for the smart system, the designed observer must have the capacity of obtaining the high-order state through output displacement of system. The extended state observer (ESO) is a kind of state observer that can get multiorders state variables of system. First, assume that a second-order system is written as (15) from (14):

$$\ddot{u}_z(t) = F(\dot{u}_z(t), u_z(t)) + bV, \tag{15}$$

where $F(\dot{u}_z(t), u_z(t)) = -2\xi\omega\dot{u}_z - \omega^2 u_z$. And (15) is written as a state equation:

$$\begin{aligned} p_1(t) &= u_z + n(t), \\ \dot{p}_1(t) &= p_2(t), \\ \dot{p}_2(t) &= p_3(t) + bV, \\ \dot{p}_3(t) &= \dot{F}(p), \end{aligned} \tag{16}$$

where $p_1(t)$ and $p_2(t)$ are states of the smart system and $n(t)$ is measurement noise.

Then, assume the two observed states (displacement and velocity) of system as $v_1$ and $v_2$ and transform them into discrete variables as

$$\begin{aligned} v_1(t+h) &= v_1(t) + hv_2(t), \\ v_2(t+h) &= v_2(t) + h \cdot \mathrm{fst}(v_1(t), v_2(t), p_1(t), r, h_1), \end{aligned} \tag{17}$$

where $h$ is time increment, and the function fst is the optical control synthesis function [32] written as

$$\begin{aligned} d &= r \cdot h_1, \\ d_0 &= d \cdot h_1, \\ e &= v_1 - p_1 + h_1 \cdot v_2, \\ a_0 &= \sqrt{d^2 + 8r|e|}, \\ a_1 &= \begin{cases} v_2 + \dfrac{e}{h_1} & |e| \le d_0, \\ v_2 + \mathrm{sgn}(e) \cdot \dfrac{a_0 - d}{2} & |e| > d_0, \end{cases} \\ \mathrm{fst}(v_1, v_2, r, h_1) &= \begin{cases} -r \cdot \dfrac{a_1}{d} & |a_1| \le d, \\ -r \cdot \mathrm{sgn}(a_1) & |a_1| > d, \end{cases} \end{aligned} \tag{18}$$

where $r$ is the initial state parameter and $h_1$ is the time increment in the fst function.

Finally, with the parameters of the designed observer in Table 2, the observed states can track the corresponding practical states of system in

$$v_1(t) \longrightarrow p_1(t), \qquad v_2(t) \longrightarrow p_2(t). \tag{19}$$

The principle diagram of ESO is shown in Figure 3. The extended state $u_z(t)$ is thought as the displacement sensed by foil gauge. By the designed observer, the online observed results are shown in Figure 4. Furthermore, Figures 4(a) and 4(b) show actual acquired displacement and the observed displacement, respectively. Compared with the actual collected

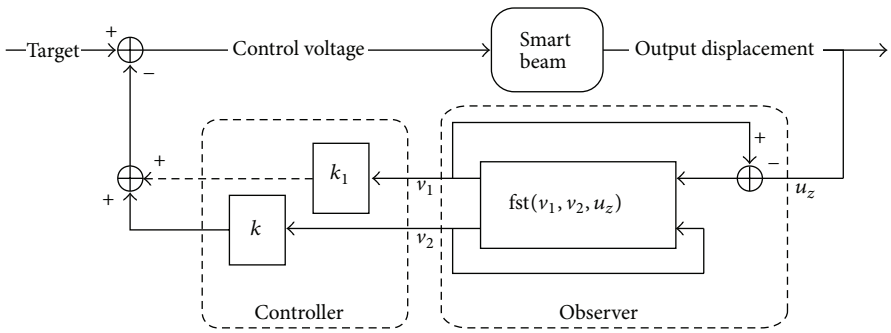


FIGURE 3: Control block.

displacement signal in Figure 4(a), the observed result signal in Figure 4(b) is filtered and becomes smoother. In addition, Figure 4(c) shows the observed velocity by the extended state observer. The amplitude of the observed velocity $v_2$ (its maximum value is $4.404 \times 10^{-5}$ m/s) is about 10 times of the amplitude of observed displacement $v_1$ (its maximum value is $3.959 \times 10^{-6}$ m).

*3.2. Controller Design.* In the paper, a state feedback control (SFC) is adopted to suppress free vibration for the smart beam. Figure 3 shows that the velocity feedback gain $k$ is much greater than the displacement feedback gain $k_1$ in the design process of SFC. Therefore, a velocity feedback controller is simplified from the SFC. In addition, the modified velocity feedback controller can increase the system's damping to attenuate the vibration faster. The control law is designed from the principle of pole placement theory. First, the target damping ratio is assumed as $\xi_o$:

$$\xi_o = \xi + \Delta, \tag{20}$$

where $\xi < \xi_o < 1$ and $\Delta$ is the quantity compensated by the velocity feedback controller.

Then, from (14), the objective system model is attained as

$$\ddot{u}_z = -\left(2\xi_o\omega_o\dot{u}_z + \omega^2 u_z\right) + bV. \tag{21}$$

As a result, the eigen matrix $A_o$ of (21) is written as

$$A_o = \lambda I - \begin{bmatrix} 0 & 1 \\ -\omega_o^2 & -2\xi_o\omega_o \end{bmatrix}, \tag{22}$$

where $\lambda$ is the eigenvalue and $I$ is the unit matrix.

To achieve the objective damping ratio $\xi_o$, the input control voltage $u_c$ in Figure 3 is designed through the state feedback control law and is expressed as

$$u_c = V = -\left(k\dot{u}_z + k_1 u_z\right). \tag{23}$$

Therefore, the close loop system is described as

$$\ddot{u}_z = -\left(2\xi\omega\dot{u}_z + \omega^2 u_z\right) - bk\dot{u}_z - bk_1 u_z. \tag{24}$$

The eigen matrix of (24) is calculated as

$$A_m = \lambda I - \begin{bmatrix} 0 & 1 \\ -\omega^2 - bk_1 & -2\xi\omega - bk \end{bmatrix}. \tag{25}$$

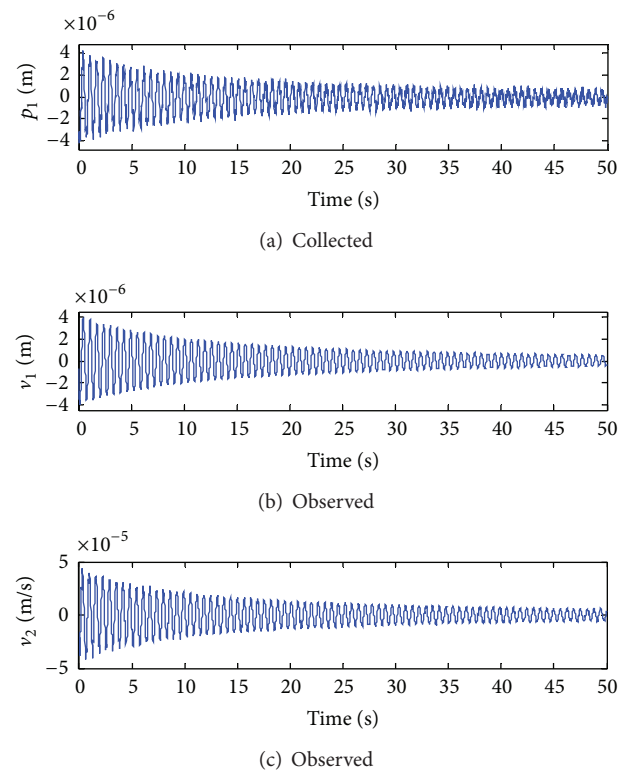


FIGURE 4: Observed and collected displacement and velocity without control.

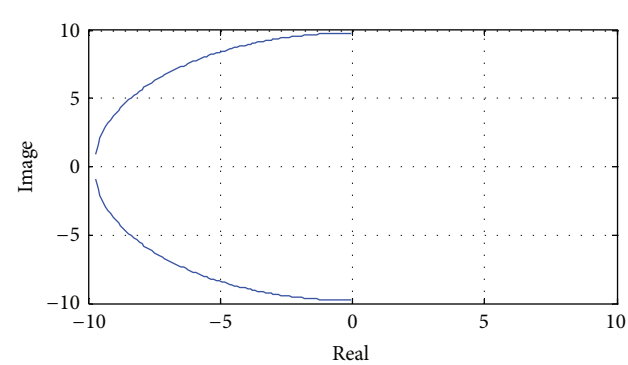


FIGURE 5: Stability analysis of velocity feedback control for smart system.

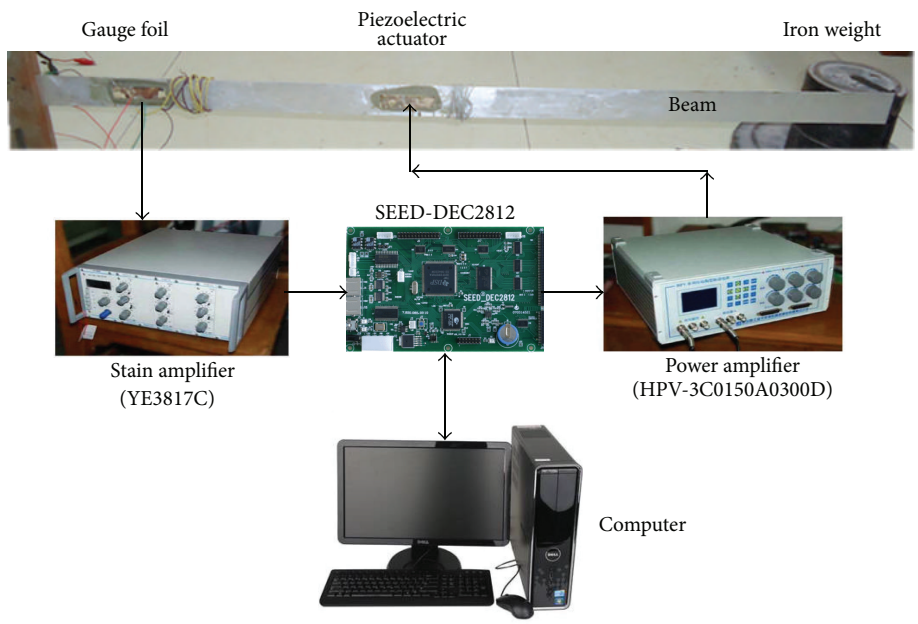


Figure 6: Experimental setup.

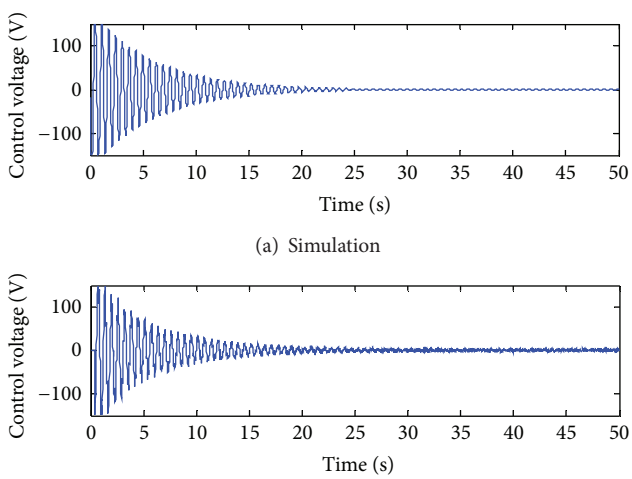


Figure 7: Control voltage.

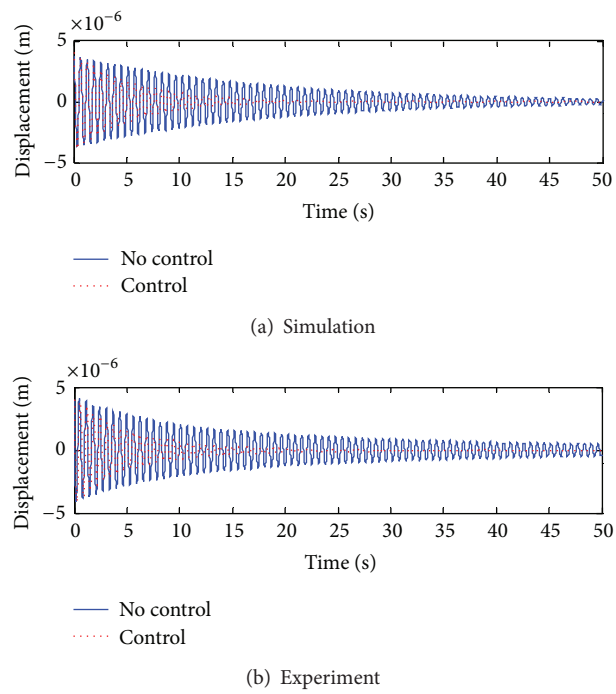


Figure 8: Control results of displacement.

Then, by pole placement theory, the eigenvalues in (22) and (25) are equal, yielding

$$|A_o| = |A_m|, \tag{26}$$

where $|\bullet|$ is determinant of the matrix.

Finally, due to (26), the state feedback gains are derived as

$$k = -\frac{2(\omega_o\xi_o - \omega\xi)}{b}, \qquad k_1 = \frac{\omega_o - \omega}{b}. \tag{27}$$

The calculated state feedback gains $k$ and $k_1$ are given in Table 2. The control voltage is attained through $k$ and $k_1$ multiplied by the displacement and velocity, respectively. However, the term $(k_1 \times v_1)$ is much less than the term $(k \times v_2)$. In other words, the control voltage is composed mainly of $(-k \times v_2)$. Therefore, a modified velocity feedback controller is simplified from the SFC to suppress vibration for the smart beam.

The stability analysis of close loop system is shown in Figure 5. The actual damping ratio $\xi$ of the close loop system

is 0.0055 without control. When the damping ratio $\xi$ is designed from 0.0055 to 1 through the modified feedback controller, the real parts of the two conjugate poles in the left side of imaginary axis increase negatively. Therefore, it is indicated that the controlled system is stable. However, the applied control voltage by the power equipment is restricted at ≤150 V; the designed damping ratio cannot be achieved up to 0.707 or even is less.

## 4. Experimental Verifications

Based on the designs of the velocity feedback control law and the extended state observer, the theoretical simulation analyses with the corresponding physical test parameters are verified by the practical experiments. Figure 6 presents the experimental setup. When the end tip of beam suffers from an initial deformation (the iron weight behind the smart beam is used for calibrating the initial disturbance loaded on the end tip of beam in each experiment), the response displacement is transformed from the strain through the gauge foil and is transferred to the control processor (SEED-DEC2812) through strain amplifier (YE3817C). The processor not only sends and saves the collected data to the computer but also receives the commands from the computer to realize the designed controller. Then by the control law the velocity feedback gain $k$ is obtained. Moreover the calculated control voltage is outputted from the processor and is applied on the piezoelectric actuator of smart beam after power amplifier (HPV-3C0150A0300D) to damp the free vibration in shorter time.

Figure 7 shows the control voltages with simulation and experiment. Before the time about 2 s, the control voltages are more than the limited voltage 150 V. Figure 8 gives the control results of displacement in simulation and experiment. After the time about 15 s, the free vibration amplitudes of displacement are all reduced up to a small value. Compared with the free vibrations without control, the control effects in simulation and experiment are obvious. Figure 9 presents the control results of velocity with simulation and experiment. It is demonstrated that the amplitudes of velocity with control are damped faster than the ones without control.

In Figures 10 and 11 in simulation and experiment, respectively, the spectrum analyses for the control results in time domain of Figures 8 and 9 are presented by Fast Fourier Transform (FFT) in MATLAB. Figures 10(a) and 10(b) give the amplitude reduction results of displacement and velocity in simulation, respectively. The two peaks with no control and with control are $1.616 \times 10^{-6}$ m and $0.5604 \times 10^{-6}$ m in Figure 10(a) while Figure 10(b) presents the peak $1.576 \times 10^{-5}$ m of curve with no control and the peak $0.5562 \times 10^{-5}$ m of curve with control. By theoretical simulation for the smart beam, it is indicated that the damping amplitudes are up to 65.32% and 64.71% in displacement and velocity, respectively.

As shown in Figure 11(a), the peaks with no control and with control in experiment are $1.5106 \times 10^{-6}$ m and $5.7215 \times 10^{-7}$ m, respectively, which indicates that the amplitudes of vibration are attenuated up to 62.13%. Figure 11(b) shows the spectrum analysis of velocity without control and with control with experiment. In addition, the peaks with no control and with control are $1.5060 \times 10^{-5}$ m/s and $5.8273 \times 10^{-6}$ m/s, respectively. Therefore, it is obvious that the reduced amplitude quantities of velocity are 61.31% in experiment.

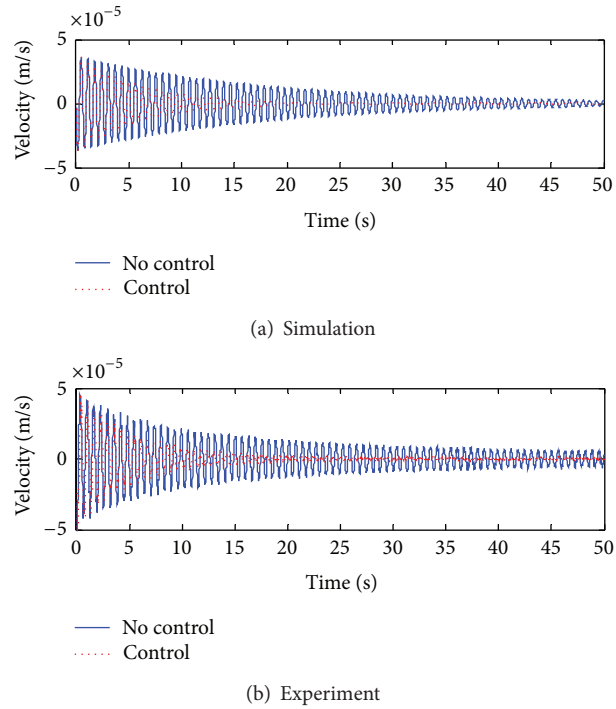


Figure 9: Control results of velocity.

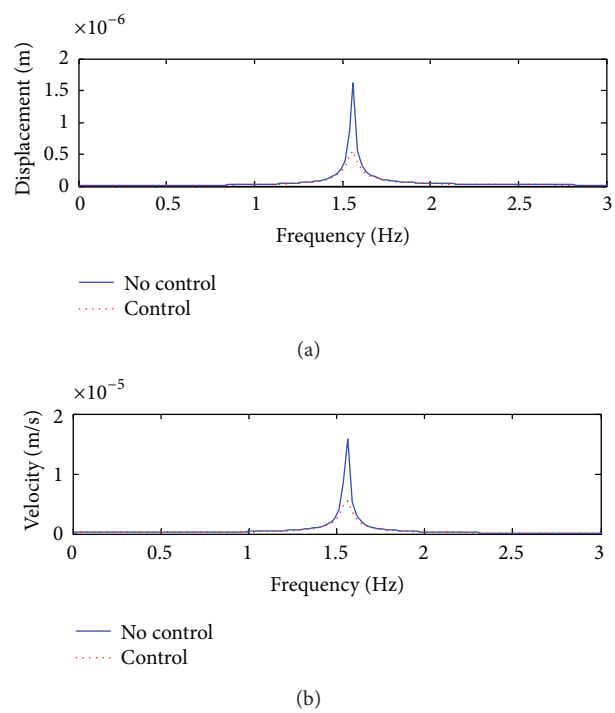


Figure 10: Spectrum analysis of control results in simulation.

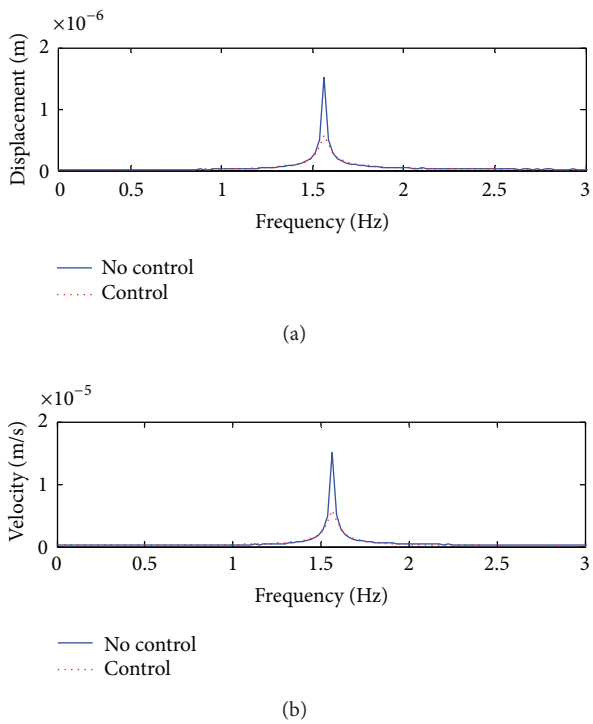


Figure 11: Spectrum analysis of control results in experiment.

In short, the simulation and experiment verifications demonstrate that the velocity feedback control with the extended state observer is feasible to suppress free vibration. Furthermore the control effects of displacement and velocity are 65.32% and 64.71%, respectively, in simulation while the control result of displacement in experiment is up to 62.13% and the control result of velocity in experiment is up to 61.31%. It is verified that the control effectiveness is considerable.

## 5. Conclusions

In this paper, the suppression vibration of a cantilevered beam bonded with a piezoelectric actuator by a velocity feedback controller with an extended state observer is focused on. The dynamical mathematical model for a smart beam is constructed using the Hamilton principle. Based on the dynamical model, the velocity feedback control is designed through the pole placement theory. The feedback velocity is obtained by an extended observer with the output displacement of the smart beam. Finally, some simulations and experiments prove that the velocity feedback control is feasible to control free vibration. Moreover, the reduced amplitudes of displacement and velocity for the smart beam are 65.32% and 64.71%, respectively, in simulation. At the same time, through the experiment verifications, the control result of displacement is up to 62.13% while the control result of velocity is up to 61.31%. It is clear that the control effectiveness is considerable and the extended state observer is useful to obtain the high-order state for the smart system.

## Appendix

Consider

$$
\begin{gathered}
B = -h_p \frac{\partial^2 \phi}{\partial x}, \\
m = \left( \int_0^{h_b} \int_0^{l_b} \rho_b w_b \phi^2 \, dx \, dz \right) \\
+ \left( \int_{h_b}^{h_b+h_p} \int_{x_p}^{x_p+l_p} \rho_p w_p \phi^2 \, dx \, dz \right), \\
k_{qq} = \int_{h_b}^{h_b+h_p} \int_{x_p}^{x_p+l_p} c_{11}^D w B^T B \, dx \, dz + \int_0^{l_b} E_b I_b \left( \frac{\partial^2 \{\phi\}}{\partial x^2} \right)^2 dx, \\
k_{Qq} = - \int_{h_b}^{h_b+h_p} \int_{x_p}^{x_p+l_p} \frac{h_{31}}{h} B \, dx \, dz, \\
k_{QQ} = \int_{h_b}^{h_b+h_p} \int_{x_p}^{x_p+l_p} \beta_{33}^x w_e \frac{1}{A_x^2} dx \, dz, \\
\alpha = \left( \int_0^{l_b} \phi \, dx \right), \qquad c = \left( \int_0^{l_b} \phi^2 dx \right) c_b, \\
\gamma = \left( \int_{x_p}^{x_p+l_p} \frac{1}{h_p} dx \right).
\end{gathered}
\tag{A.1}
$$

## Conflict of Interests

The authors declare that there is no conflict of interests regarding the publication of this paper.

## Acknowledgment

This work was funded by the National Natural Science Foundation of China, under Grant no. 11072148.

## References

[1] V. Fakhari and A. Ohadi, "Nonlinear vibration control of functionally graded plate with piezoelectric layers in thermal environment," *Journal of Vibration and Control*, vol. 17, no. 3, pp. 449–469, 2011.

[2] H. Gu and G. Song, "Active vibration suppression of a flexible beam with piezoceramic patches using robust model reference control," *Smart Materials and Structures*, vol. 16, no. 4, pp. 1453–1459, 2007.

[3] M. Marinaki, Y. Marinakis, and G. E. Stavroulakis, "Fuzzy control optimized by a multi-objective particle swarm optimization algorithm for vibration suppression of smart structures," *Structural and Multidisciplinary Optimization*, vol. 43, no. 1, pp. 29–42, 2011.

[4] O. Bilgen, M. Amin Karami, D. J. Inman, and M. I. Friswell, "The actuation characterization of cantilevered unimorph beams with single crystal piezoelectric materials," *Smart Materials and Structures*, vol. 20, no. 5, Article ID 055024, 2011.

[5] D. Ezhilarasi, M. Umapathy, and B. Bandyopadhyay, "Design and experimental evaluation of simultaneous periodic output feedback control for piezoelectric actuated beam structure," *Structural Control and Health Monitoring*, vol. 16, no. 3, pp. 335–349, 2009.

[6] Z. C. Qiu, "Adaptive nonlinear vibration control of a Cartesian flexible manipulator driven by a ballscrew mechanism," *Mechanical Systems and Signal Processing*, vol. 30, pp. 248–266, 2012.

[7] G. Meng, L. Ye, X. Dong, and K. Wei, "Closed loop finite element modeling of piezoelectric smart structures," *Shock and Vibration*, vol. 13, no. 1, pp. 1–12, 2006.

[8] M. Dadfarnia, N. Jalili, Z. Liu, and D. M. Dawson, "An observer-based piezoelectric control of flexible Cartesian robot arms: theory and experiment," *Control Engineering Practice*, vol. 12, no. 8, pp. 1041–1053, 2004.

[9] C. M. A. Vasques and J. Dias Rodrigues, "Active vibration control of a smart beam through piezoelectric actuation and laser vibrometer sensing: simulation, design and experimental implementation," *Smart Materials and Structures*, vol. 16, no. 2, pp. 305–316, 2007.

[10] V. Sethi and G. Song, "Multimodal vibration control of a flexible structure using piezoceramic sensor and actuator," *Journal of Intelligent Material Systems and Structures*, vol. 19, no. 5, pp. 573–582, 2008.

[11] D. Ezhilarasi, M. Umapathy, and B. Bandyopadhyay, "Design and experimental evaluation of piecewise output feedback control for structural vibration suppression," *Smart Materials and Structures*, vol. 15, no. 6, pp. 1927–1938, 2006.

[12] Z.-C. Qiu, J.-D. Han, X.-M. Zhang, Y. Wang, and Z. Wu, "Active vibration control of a flexible beam using a non-collocated acceleration sensor and piezoelectric patch actuator," *Journal of Sound and Vibration*, vol. 326, no. 3–5, pp. 438–455, 2009.

[13] S. N. Mahmoodi and M. Ahmadian, "Modified acceleration feedback for active vibration control of aerospace structures," *Smart Materials and Structures*, vol. 19, no. 6, Article ID 065015, 10 pages, 2010.

[14] A. Zabihollah, R. Sedagahti, and R. Ganesan, "Active vibration suppression of smart laminated beams using layerwise theory and an optimal control strategy," *Smart Materials and Structures*, vol. 16, no. 6, pp. 2190–2201, 2007.

[15] S. M. Khot, N. P. Yelve, R. Tomar, S. Desai, and S. Vittal, "Active vibration control of cantilever beam by using PID based output feedback controller," *Journal of Vibration and Control*, vol. 18, no. 3, pp. 366–372, 2012.

[16] Q. Hu, J. Cao, and Y. Zhang, "Robust backstepping sliding mode attitude tracking and vibration damping of flexible spacecraft with actuator dynamics," *Journal of Aerospace Engineering*, vol. 22, no. 2, pp. 139–152, 2009.

[17] K. Gurses, B. J. Buckham, and E. J. Park, "Vibration control of a single-link flexible manipulator using an array of fiber optic curvature sensors and PZT actuators," *Mechatronics*, vol. 19, no. 2, pp. 167–177, 2009.

[18] Y. Zhang, X. Zhang, and S. Xie, "Adaptive vibration control of a cylindrical shell with laminated PVDF actuator," *Acta Mechanica*, vol. 210, no. 1-2, pp. 85–98, 2010.

[19] Q. Hu, "Robust adaptive attitude tracking control with L2-gain performance and vibration reduction of an orbiting flexible spacecraft," *Journal of Dynamic Systems, Measurement and Control, Transactions of the ASME*, vol. 133, no. 1, Article ID 011009, 11 pages, 2011.

[20] H. Ji, J. Qio, A. Badel, and K. Zhu, "Semi-active vibration control of a composite beam using an adaptive SSDV approach," *Journal of Intelligent Material Systems and Structures*, vol. 20, no. 4, pp. 401–412, 2009.

[21] H. Ji, J. Qiu, A. Badel, Y. Chen, and K. Zhu, "Semi-active vibration control of a composite beam by adaptive synchronized switching on voltage sources based on LMS algorithm," *Journal of Intelligent Material Systems and Structures*, vol. 20, no. 8, pp. 939–947, 2009.

[22] M. Ahmadian and D. J. Inman, "Adaptive modified positive position feedback for active vibration control of structures," *Journal of Intelligent Material Systems and Structures*, vol. 21, no. 6, pp. 571–580, 2010.

[23] J. Lin and W. S. Chao, "Vibration suppression control of beam-cart system with piezoelectric transducers by decomposed parallel adaptive neuro-fuzzy control," *JVC/Journal of Vibration and Control*, vol. 15, no. 12, pp. 1885–1906, 2009.

[24] Q. L. Hu, "Robust adaptive sliding mode attitude control and vibration damping of flexible spacecraft subject to unknown disturbance and uncertainty," *Transactions of the Institute of Measurement and Control*, vol. 34, no. 4, pp. 436–447, 2012.

[25] X. Xue and J. Tang, "Robust and high precision control using piezoelectric actuator circuit and integral continuous sliding mode control design," *Journal of Sound and Vibration*, vol. 293, no. 1-2, pp. 335–359, 2006.

[26] D. Sun, J. K. Mills, J. Shan, and S. K. Tso, "A PZT actuator control of a single-link flexible manipulator based on linear velocity feedback and actuator placement," *Mechatronics*, vol. 14, no. 4, pp. 381–401, 2004.

[27] J. Roos, J. C. Bruch Jr., J. M. Sloss, S. Adali, and I. S. Sadek, "Velocity feedback control with time delay using piezoelectrics," in *Proceedings of the SPIE The International Society for Optical Engineering: smart Structures and Materials 2003 Modeling, Signal Processing, and Control*, vol. 5049, pp. 233–240, March 2003.

[28] P. Gardonio and S. J. Elliott, "Smart panels with velocity feedback control systems using triangularly shaped strain actuators," *Journal of the Acoustical Society of America*, vol. 117, no. 4, pp. 2046–2064, 2005.

[29] Y. Huang and J. Han, "Analysis and design for the second order nonlinear continuous extended states observer," *Chinese Science Bulletin*, vol. 45, no. 21, pp. 1938–1944, 2000.

[30] A. J. Hillis, "Active motion control of fixed offshore platforms using an extended state observer," *Proceedings of the Institution of Mechanical Engineers I*, vol. 224, no. 1, pp. 53–63, 2010.

[31] R. Zhang and C. Tong, "Torsional vibration control of the main drive system of a rolling mill based on an extended state observer and linear quadratic control," *Journal of Vibration and Control*, vol. 12, no. 3, pp. 313–327, 2006.

[32] Y. Dong, M. X. Jun, and C. Hua, "Realization of DESO filter on DSP and its application," *Journal of Academy of Armored Force Engineering*, vol. 24, no. 3, pp. 57–61, 2010.